IEEE Access
Multidisciplinary | Rapid Review | Open Access Journal

Received October 8, 2020, accepted October 18, 2020, date of publication October 22, 2020, date of current version November 10, 2020.

Digital Object Identifier 10.1109/ACCESS.2020.3033055

Joint Hybrid Precoder and Combiner for Wideband Millimeter-Wave Massive MIMO Systems

TALHA MIR[1], (Member, IEEE), UBAID ABBASI[2], RAZA ALI[1], (Member, IEEE), SYED MUDASSIR HUSSAIN[1], (Member, IEEE), AND USAMA MIR[3], (Senior Member, IEEE)

[1]Department of Electronic Engineering, Balochistan University of Information Technology, Engineering, and Management Sciences, Quetta 87300, Pakistan
[2]Department of Sciences, GPRC, Grande Prairie, AB T8V 4C4, Canada
[3]Saudi Electronic University (SEU), Riyadh 11673, Saudi Arabia

Corresponding author: Usama Mir (u.mir@seu.edu.sa)

ABSTRACT Hybrid precoding and combining is a key technique to provide an appropriate antenna gain in millimeter-wave (mmWave) massive multiple-input multiple-output (MIMO) systems. In wideband mmWave channels, the analog precoder and combiner is designed in the time domain and remain unchanged over the whole bandwidth. In contrast, digital precoders and combiners are optimized on a per-subcarrier basis which makes the resultant problem very difficult. To solve this problem, we combine the well-known turbo-equalizer with the tabu-search (TS)-algorithm developed in artificial intelligence and propose TS-based joint hybrid precoding and combining scheme to intelligently search the near-optimum pair of hybrid precoder and combiner. Specifically, our scheme consists of two key steps. At first, a base station (BS) and a mobile station (MS) develop the turbo-like (TL)-joint search by using the idea of iterative information exchange between them. Then, to find out the near-optimum pair of hybrid precoder and combiner in each iteration of the TL-joint search, the TS-algorithm is employed. Simulation results are shown to verify the significant sum-rate performance of the proposed solution with low-complexity compared to some existing solutions.

INDEX TERMS Hybrid precoding, millimeter-wave, massive MIMO, artificial intelligence.

I. INTRODUCTION

Due to the continuous growth in data-rate requirements of the current cellular networks, new spectrum resources are needed to explore [1]. The rich and unexplored spectrum resources at millimeter-wave (mmWave) frequencies make mmWave band suitable option to satisfy the increasing data rate demand of these cellular networks [2]. However, mmWave signals have severe propagation loss [3] and thus are very sensitive to the blockage problem due to the very short wavelengths associated with them [4]. To overcome this loss, a large antenna array turns out to be a feasible solution. Short wavelengths of mmWave signals enable to employ the large antenna array in the compact form [5]. Multiple-input-multiple-output (MIMO) in low-frequency range (e.g., 2-3 GHz) use fully-digital precoding to achieve the sufficient array gain in order to avoid path-loss [6]. To employ the fully-digital precoding, a dedicated radio-frequency (RF) chain is required at each antenna [7]. For large antenna systems (e.g., 256 antennas and above), this traditional fully-digital precoding cannot be used due to the large number of required RF chains as RF chains are power-hungry and expensive [8]. Therefore, it is not a trivial task to design the transceivers for mmWave massive MIMO systems [9].

To reduce the hardware cost and complexity, hybrid (analog and digital) precoding has been proposed recently [10]. In hybrid precoding, the large-size conventional digital precoder is divided into two parts [11]. One is the small-size digital precoder realized by the small number of RF chains to cancel the interference. The other part is the large-size analog precoder implemented by using the phase shifters or switches to increase the antenna gain [12]. In this way, hybrid precoding is capable to inherit the sum-rate performance close to the fully-digital precoding and also significantly reduce the number of required RF chains [4].

The associate editor coordinating the review of this manuscript and approving it for publication was Ting Li.

A. RELATED WORK

In recent years, hybrid precoding has drawn a lot of attention for mmWave massive MIMO systems. The idea of hybrid precoding was first presented in [13] for single-user MIMO systems. Then, in [10] the authors formulated the sum-rate maximization problem for hybrid precoding as matrix factorization and proposed the orthogonal-matching-pursuit (OMP)-algorithm. The authors in [14] used the same formulated problem as in [10] and proposed an alternating-minimization (AM)-algorithm. Beside OMP and AM, the authors in [15], [16], and [17] also proposed effective solutions to solve the hybrid precoding problem. However, all these solutions considered the narrowband mmWave channels. Moreover, it is claimed that the mmWave systems are more likely to be deployed in wideband scenarios because of the large available bandwidth of mmWave signals (e.g., 2 GHz) [5].

For conventional fully-digital precoding, it is easy to extend from narrowband to wideband by simply employing the orthogonal frequency division multiplexing (OFDM) (i.e., by converting the frequency-selective wideband channel into a series of frequency-flat subchannels) [18]. However, this simple extension cannot work for hybrid precoding. In hybrid precoding, the digital precoder is realized by RF chains and it has to be designed on per-subcarrier basis. Conversely, the network of phase-shifters is used to implement the analog precoder and it needs to be designed by considering the entire wideband [18]. This distinct feature of hybrid precoding for wideband mmWave channels makes it more challenging compared to the conventional fully-digital precoding [19].

In the current literature, compared to narrowband hybrid precoding, wideband hybrid precoding has only a few examples. For example, the authors in [20] focus on the spectral efficiency maximization for wideband mmWave systems. They provide the codebook design guidelines at first for wideband mmWave channels and then propose the gram-Schmidt-orthogonalization algorithm to solve the hybrid precoding problem. Likewise, in [21], a closed-form solution for the hybrid precoding problem is proposed with a dynamic sub-array structure. Although, the works in [20] and [21] are very effective to solve the hybrid precoding problem for wideband mmWave channels, but they completely neglect the impact of hybrid combiner while optimizing the hybrid precoder. Nevertheless, it is still necessary to study the impact of the joint design of a hybrid precoder and a hybrid combiner for a wideband mmWave massive MIMO system. This encourages us to fill in the aforementioned important research gap by proposing a joint optimization of hybrid precoder and combiner for wideband mmWave massive MIMO systems.

B. OUR CONTRIBUTIONS

To reduce the searching complexity of beamforming for mmWave communications, some low-complexity schemes have already been proposed. These schemes can reduce the searching complexity without obvious performance loss. However, they usually involve a large number of iterations to exchange the information between the user and the BS, leading to a high overhead, especially when the size of codebook is large. Further, as stated above, we propose low-complexity joint hybrid precoding and combining scheme to obtain a near-optimum pair of hybrid precoder and combiner for wideband mmWave massive MIMO systems. In our work, the digital precoder is designed on a per-subcarrier basis and the analog precoder is designed by considering it as subcarrier-independent for the whole bandwidth. Then, under some practical constraints (e.g., total power and constant modulus), the joint hybrid precoding and combining optimization problem is formulated to maximize the achievable sum-rate.

To solve the sum-rate maximization problem, we utilize the idea of turbo-like (TL) joint search and combine it with a tabu-search (TS) algorithm to a propose TS-based joint hybrid precoding and combining scheme. The proposed scheme work as follows.

At first, the TL-joint search between the base station (BS) and the mobile station (MS) is developed which iteratively exchanges the information between BS and MS and search the near-optimal pair of hybrid precoder and combiner. Different from conventional TL-like scheme [22] where the TL-search starts by selecting a random initial solution from the predefined codebook, we propose an initialization procedure based on eigenvalue decomposition (EVD) of the effective channel to obtain the initial hybrid precoder and combiner.

Next, our scheme combines the TL-joint search with TS-algorithm to intelligently look for the best pair of hybrid precoder and combiner with low-complexity in each interaction between the BS and the MS. Compared to [22], our algorithm proves to be simple in order to find the exact initial solution to start the TS-algorithm.

We also provide some important definitions (e.g., neighborhood, cost function, and stopping criterion) which are helpful to understand the TS-based joint hybrid precoding and combining. Further, we provide a complexity analysis of the proposed scheme. Finally, the simulation results show that the proposed solution can achieve the higher sum-rate as compared to some existing solutions [14], [16].

C. ORGANIZATION AND NOTATION

The remaining part of this paper is organized as follows. In Section II, we present the system and channel models used for wideband mmWave massive MIMO systems. Section III provides the sum-rate maximization problem under some practical constraints. In Section IV, we first introduce the TL-joint search, combine it with TS-algorithm, and then propose the TS-based joint hybrid precoding and combining scheme. Section V provides some important definitions and the complexity analysis of the proposed scheme. Simulation results are explained in Section VI. Finally, Section VII concludes our paper.

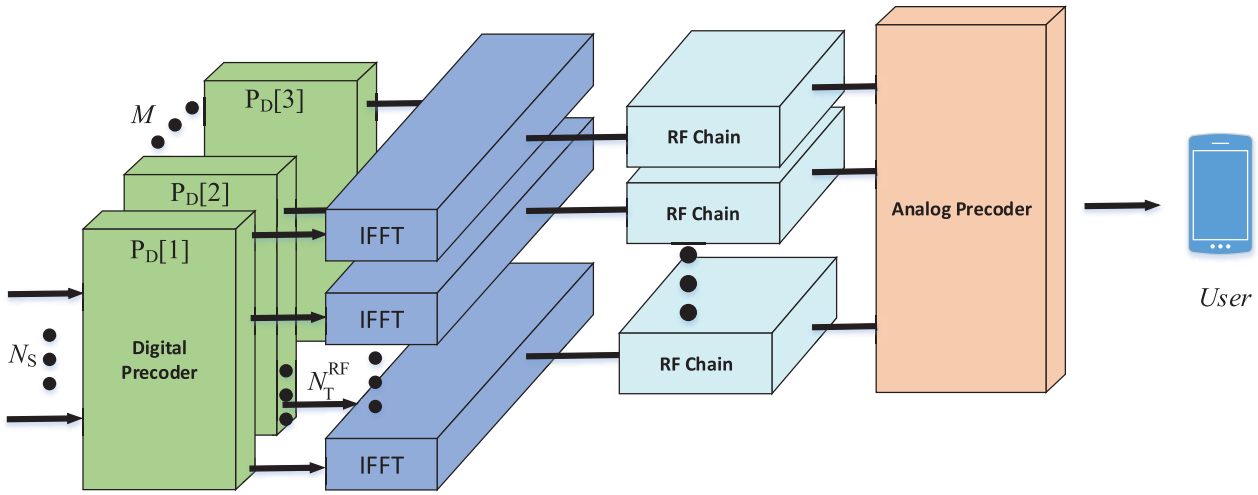

FIGURE 1. Hybrid precoding for wideband mmWave massive MIMO systems.

Notations: Uppercase and Lowercase boldface letters represent matrices and vectors, respectively; $(\cdot)^T$, $(\cdot)^H$, $(\cdot)^{-1}$, and $\det(\cdot)$ are the transpose, conjugate transpose, inversion, and determinant of the matrix, respectively. $\mathcal{CN}\left(0,\sigma^2\right)$ denotes the zero-mean complex Gaussian distribution and the variance σ^2. Finally, $\mathbf{I}_N$ is the $N \times N$ identity matrix.

II. SYSTEM AND CHANNEL MODELS

This section presents the system and channel models of hybrid precoding for wideband mmWave massive MIMO systems.

A. SYSTEM MODEL

As shown in Fig. 1, we consider hybrid precoding for massive MIMO-OFDM systems over wideband mmWave channels with K subcarriers. The BS is equipped with N_{T} transmit antennas and N_{T}^{RF} RF chains. The BS transmits N_s data streams simultaneously to the MS equipped with N_{R} receive antennas and N_{R}^{RF} RF chains. We set $N_{RF} \leqslant N_T \leqslant N_s$ where $N_{\mathrm{R}}^{RF} = N_{\mathrm{T}}^{RF} = N_{\mathrm{s}}$ to achieve the spatial multiplexing gain [20].

At the BS, N_s data-symbols $\mathbf{s}[k]$ at each subcarrier k (where $k = 1,\cdots,K$) are first precoded with a subcarrier-dependent digital precoder $\mathbf{F}_{\mathrm{BB}}[k]$ of size $N_{\mathrm{T}}^{RF} \times N_s$. Then, by using K-point inverse fast-fourier transform (IFFT), the data-symbols are transformed to the time domain. A cyclic prefix (CP) of length D is then added to the data-symbols and finally the analog precoder $\mathbf{F}_{\mathrm{RF}}$ of size $N_{\mathrm{T}} \times N_{\mathrm{T}}^{RF}$ is applied. It should be emphasized that the subcarrier-independent analog precoder $\mathbf{F}_{\mathrm{RF}}$ is realized in time domain, and it remains unchanged over all the subcarriers. In contrast, the digital precoder $\mathbf{F}_{\mathrm{BB}}[k]$ is subcarrier dependent and performed in frequency domain. This is the key difference between the wideband hybrid precoding and the conventional OFDM-based fully digital precoding where the digital precoder is subcarrier dependent. The transmitted signal at kth subcarrier can be written as [10]:

$$\mathbf{x}[k] = \mathbf{F}_{\mathrm{RF}}\mathbf{F}_{\mathrm{BB}}[k]\,\mathbf{s}[k], \tag{1}$$

where $\mathbf{s}[k]$ is the $N_s \times 1$ transmitted vector at kth subcarrier with $\mathbb{E}\left[\mathbf{s}[k]\mathbf{s}[k]^H\right] = \mathbf{I}_{N_s}$. Usually, the analog precoder is realized by the network of phase shifters, therefore its entries satisfy the constant modulus constraint. We normalize the entries of analog precoder as $\left|[\mathbf{F}_{\mathrm{RF}}]_{i,j}\right|^2 = 1$. Moreover, the $\mathbf{F}_{\mathrm{RF}}$ and $\mathbf{F}_{\mathrm{BB}}[k]$ are coupled together through the total transmit power constraint as $\sum_{k=1}^{K}\|\mathbf{F}_{\mathrm{RF}}\mathbf{F}_{\mathrm{BB}}[k]\|_F^2 \leq P_{tot}$, where P_{tot} is the total transmitted power.

At the MS, perfect carrier and frequency offset synchronization is considered. The received signal is combined first with an analog combiner $\mathbf{W}_{\mathrm{RF}}$ of size $N_{\mathrm{R}} \times N_{\mathrm{R}}^{RF}$ in analog domain. Then, the CP is removed, and the data-symbols are returned back to the frequency domain by using K-FFT's. Finally, the data-symbols at each subcarrier k are combined by the digital combiner $\mathbf{W}_{\mathrm{BB}}[k]$ of size $N_{\mathrm{R}}^{RF} \times N_s$. The overall received signal at kth subcarrier can be expressed as [10]:

$$\begin{aligned}\mathbf{y}[k] =& \mathbf{W}_{\mathrm{BB}}^H[k]\,\mathbf{W}_{\mathrm{RF}}^H\mathbf{H}[k]\,\mathbf{F}_{\mathrm{RF}}\mathbf{F}_{\mathrm{BB}}[k]\,\mathbf{s}[k] \\ &+\mathbf{W}_{\mathrm{BB}}^H[k]\,\mathbf{W}_{\mathrm{RF}}^H\mathbf{n}[k],\end{aligned} \tag{2}$$

where $\mathbf{H}[k]$ is the channel matrix between the BS and the MS at kth subcarrier, and $\mathbf{n}[k] \sim \mathcal{CN}\left(0,\sigma^2\mathbf{I}_{N_s}\right)$ is the additive white Gaussian noise vector with independent and identical distribution. Then, by denoting

$$\mathbf{F}_{\mathrm{RF}}\mathbf{F}_{\mathrm{BB}}[k] = \mathbf{F}_{\mathrm{T}}[k], \tag{3a}$$

$$\mathbf{W}_{\mathrm{RF}}\mathbf{W}_{\mathrm{BB}}[k] = \mathbf{W}_{\mathrm{R}}[k], \tag{3b}$$

as the overall hybrid precoding and combining matrix for the kth subcarrier, (2) can be written as:

$$\mathbf{y}[k] = \mathbf{W}_{\mathrm{R}}^H[k]\,\mathbf{H}[k]\,\mathbf{F}_{\mathrm{T}}[k]\,\mathbf{s}[k] + \mathbf{W}_{\mathrm{R}}^H[k]\,\mathbf{n}[k]. \tag{4}$$

B. CHANNEL MODEL

Due to the limited number of dominant paths in mmWave channels, the widely used geometric channel model is adopted in this paper. There are L clusters and each cluster l ($1 \le l \le L$) has a time delay $\tau_l \in \mathbb{R}$, and angle of arrival and departure (AoA/AoD) $\theta_l, \phi_l \in [0, 2\pi]$, respectively. Further, each cluster l contributes R_l rays between the BS and the MS. Each ray r_l ($1 \le r_l \le R_l$) has relative time delay τ_{rl}, relative AoA/AoD shift υ_{rl}, φ_{rl}, and complex path gain α_{rl}. Furthermore, p_{pl} presents the path-loss between the BS and the MS, and $p_{rc}(\tau)$ is a pulse-shaping function for T_s-spaced signal at τ seconds. The delay-d MIMO channel model $\mathbf{H}[d]$ can be expressed as [10]:

$$\mathbf{H}[d] = \sqrt{\frac{N_{\mathrm{T}}N_{\mathrm{R}}}{p_{pl}}} \sum_{l=1}^{L} \sum_{r_l=1}^{R_l} \alpha_{rl} p_{rc}(dT_s - \tau_l - \tau_{rl}) \times \mathbf{a}_{\mathrm{MS}}(\theta_l - \upsilon_{lr})\, \mathbf{a}^*_{\mathrm{BS}}(\phi_l - \varphi_{lr}), \quad (5)$$

where $\mathbf{a}_{\mathrm{MS}}(\cdot)$ and $\mathbf{a}_{\mathrm{BS}}(\cdot)$ are the antenna array response vectors depending on the antenna array structure at the BS and the MS. If we adopt the widely used uniform linear array (ULA), then we have:

$$\mathbf{a}_{\mathrm{BS}}(\theta_l) = \frac{1}{\sqrt{N_t}} \times \left[1, e^{j2\pi\lambda^{-1}d_s\sin(\theta_l)}, \ldots, e^{j(N_t-1)2\pi\lambda^{-1}d_s\sin(\theta_l)}\right]^T, \quad (6a)$$

$$\mathbf{a}_{\mathrm{MS}}(\phi_l) = \frac{1}{\sqrt{N_t}} \times \left[1, e^{j2\pi\lambda^{-1}d_s\sin(\phi_l)}, \ldots, e^{j(N_r-1)2\pi\lambda^{-1}d_s\sin(\phi_l)}\right]^T, \quad (6b)$$

where λ is the wavelength of the signal, d_s is the antenna spacing which is usually $d_s = \lambda/2$, and D is the CP length. Given the delay-d channel model in (5), the channel at kth subcarrier between the BS and the MS can be written as [10]:

$$\mathbf{H}[k] = \sum_{d=0}^{D-1} \mathbf{H}[d] e^{-j\frac{2\pi k}{K}d}. \quad (7)$$

III. PROBLEM FORMULATION

Based on the above system and channel models, in this section, we present the codebook based hybrid precoding which is commonly used in mmWave massive MIMO systems. Then, the sum-rate maximization problem is formulated for the considered system under some practical constraints.

A. CODEBOOK-BASED HYBRID PRECODING

The beamsteering-codebook is the most common analog codebook used for mmWave channels [23]. The analog precoder and combiner beamsteering codebooks can be presented by $\mathcal{F}$ and $\mathcal{W}$, respectively. If B_{T}^{RF} (B_{R}^{RF}) bits are used to quantify the angle of arrival and departure, respectively, then codebooks $\mathcal{F}$ ($\mathcal{W}$) will contain all the possible matrices of $\mathbf{F}_{\mathrm{RF}}$ ($\mathbf{W}_{\mathrm{RF}}$) which can be expressed as [24]:

$$\mathbf{F}_{\mathrm{RF}} = \left[\mathbf{a}_{\mathrm{BS}}\left(\bar{\phi}_1^{\mathrm{BS}}\right), \mathbf{a}_{\mathrm{BS}}\left(\bar{\phi}_2^{\mathrm{BS}}\right), \ldots, \mathbf{a}_{\mathrm{BS}}\left(\bar{\phi}_{N_{\mathrm{T}}^{RF}}^{\mathrm{BS}}\right)\right], \quad (8a)$$

$$\mathbf{W}_{\mathrm{RF}} = \left[\mathbf{a}_{\mathrm{MS}}\left(\bar{\theta}_1^{\mathrm{MS}}\right), \mathbf{a}_{\mathrm{MS}}\left(\bar{\theta}_2^{\mathrm{MS}}\right), \ldots, \mathbf{a}_{\mathrm{MS}}\left(\bar{\theta}_{N_{\mathrm{R}}^{RF}}^{\mathrm{MS}}\right)\right], \quad (8b)$$

where the quantified AoD $\bar{\phi}_i^{\mathrm{BS}}$ for ($i = 1, \cdots, N_{\mathrm{T}}^{RF}$) at the BS has $2^{B_{\mathrm{T}}^{RF}}$ possible entries, (i.e., $\bar{\phi}_i^{\mathrm{BS}} = 2\pi n \big/ 2^{B_{\mathrm{T}}^{RF}}$) where $n \in \left\{1, \cdots, 2^{B_{\mathrm{T}}^{RF}}\right\}$.

Similarly, the quantified AoA $\bar{\theta}_j^{\mathrm{MS}}$ for ($j = 1, \cdots, N_{\mathrm{R}}^{RF}$) at the MS has $2^{B_{\mathrm{R}}^{RF}}$ possible choices, (i.e., $\bar{\theta}_j^{\mathrm{MS}} = 2\pi n \big/ 2^{B_{\mathrm{R}}^{RF}}$) where $n \in \left\{1, \cdots, 2^{B_{\mathrm{R}}^{RF}}\right\}$. Therefore, the cardinalities $|\mathcal{F}|$ and $|\mathcal{W}|$ of $\mathcal{F}$ and $\mathcal{W}$ can be expressed as $2^{B_{\mathrm{T}}^{RF}.N_{\mathrm{T}}^{RF}}$ and $2^{B_{\mathrm{R}}^{RF}.N_{\mathrm{R}}^{RF}}$, respectively.

B. PROBLEM FORMULATION

The main focus of this paper is to find out the near-optimum pair of hybrid precoder and combiner which maximizes the achievable sum-rate of the system. Therefore, given the received signal in (4), the achievable sum-rate R can be expressed as:

$$R[k] = \log_2 \left| \mathbf{I}_{N_{\mathrm{s}}} + \frac{\rho}{N_{\mathrm{s}}} \mathbf{R}_n^{-1}[k][\mathbf{W}_{\mathrm{R}}[k]]^H \mathbf{H}[k]\, \mathbf{F}_{\mathrm{T}}[k] [\mathbf{F}_{\mathrm{T}}[k]]^H [\mathbf{H}[k]]^H \mathbf{W}_{\mathrm{R}}[k] \right|, \quad (9)$$

where $\mathbf{R}_n^{-1}[k] = \sigma^2 [\mathbf{W}_{\mathrm{R}}[k]]^H \mathbf{W}_{\mathrm{R}}[k]$ is the noise covariance matrix after combining. Then,

$$\varphi(\mathbf{F}_{\mathrm{T}}[k], \mathbf{W}_{\mathrm{R}}[k]) = \left| \mathbf{I}_{N_{\mathrm{s}}} + \frac{\rho}{N_{\mathrm{s}}} \mathbf{R}_n^{-1}[k][\mathbf{W}_{\mathrm{R}}[k]]^H \mathbf{H}[k]\, \mathbf{F}_{\mathrm{T}}[k] [\mathbf{F}_{\mathrm{T}}[k]]^H [\mathbf{H}[k]]^H \mathbf{W}_{\mathrm{R}}[k] \right|, \quad (10)$$

where $\varphi(\mathbf{F}_{\mathrm{T}}[k], \mathbf{W}_{\mathrm{T}}[k])$ is the cost function. Our target is to jointly design the hybrid precoder and combiner to maximize the sum-rate R. This problem can be formulated as:

$$\begin{aligned} &\left\{\mathbf{F}_{\mathrm{RF}}^*, \mathbf{F}_{\mathrm{BB}}^*[k], \mathbf{W}_{\mathrm{RF}}^*, \mathbf{W}_{\mathrm{BB}}^*[k]\right\} \\ &= \arg\max R \\ &\quad \text{s.t. } \mathbf{F}_{\mathrm{RF}}(i,j) \in \mathcal{F}, \quad \forall i,j \\ &\quad\quad \mathbf{W}_{\mathrm{RF}}(i,j) \in \mathcal{W}, \quad \forall i,j \\ &\quad\quad \sum_{k=1}^{K} \|\mathbf{F}_{\mathrm{RF}}\mathbf{F}_{\mathrm{BB}}[k]\|_F^2 = N_s \end{aligned} \quad (11)$$

The optimization problem (11) is hard to solve due to the non-convex constraints and coupling variables. In the next section, we propose a low-complexity TS-based joint hybrid precoding and combining scheme to solve this problem.

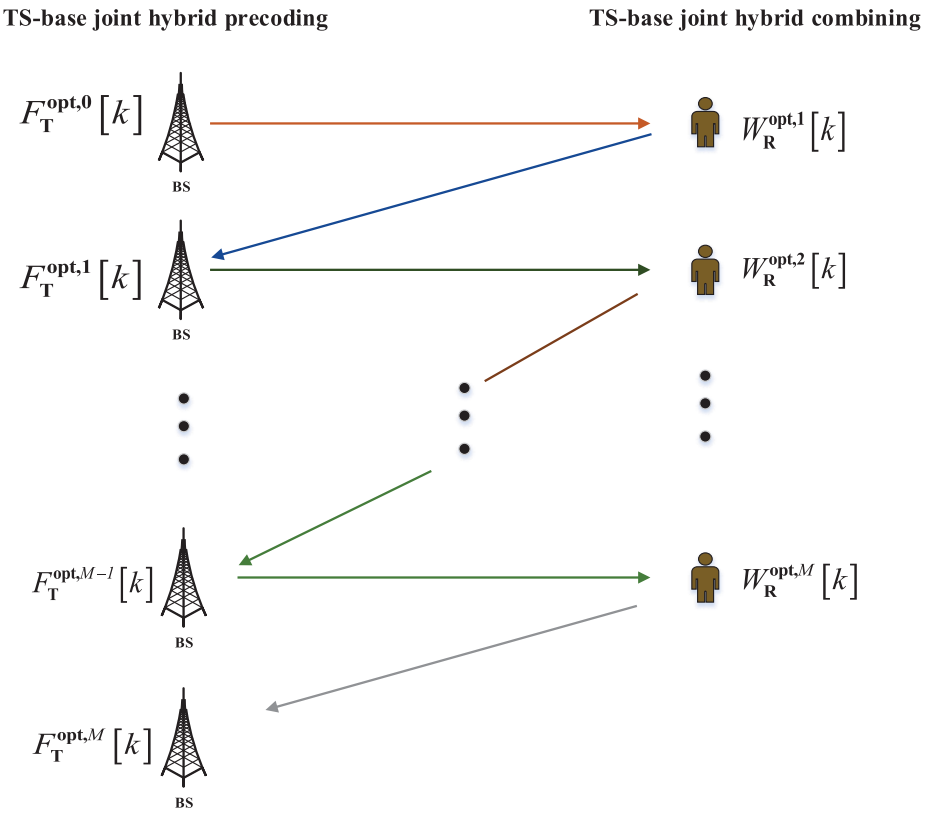

FIGURE 2. Turbo-like joint searching between the BS and the MS.

IV. TABU SEARCH-BASED JOINT HYBRID PRECODING/COMBINING

Our proposed scheme is composed of two key steps. At first, we design the TL-joint search based on the iterative information exchange between the BS and the MS to obtain a near-optimum pair of hybrid precoder and combiner. Then, in each iteration of the TL-joint search, we utilize the TS-algorithm to search the best pair of hybrid precoder and combiner from the given codebooks with low-complexity.

A. TL-JOINT SEARCH

Inspired by the idea of information exchange between the BS and the MS in well known turbo-equalizer, we first design the TL-joint search to find a near-optimum pair of hybrid precoder and combiner as depicted in Fig. 2. Let $\mathbf{F}_{\mathrm{T}}^{\mathrm{opt,m}}[k]$ and $\mathbf{W}_{\mathrm{R}}^{\mathrm{opt,m}}[k]$ are the near-optimum pair of hybrid precoder and combiner obtained till mth iteration (M is the predefined maximum iterations). In conventional TL-search [22], the BS at first selects a random initial hybrid precoder $\mathbf{F}_{\mathrm{T}}^{\mathrm{opt},0}[k]$ from the codebook $\mathcal{F}$ and transmits the training sequence to the MS. Subsequently, based on the received information from the BS, the MS searches best hybrid combiner $\mathbf{W}_{\mathrm{R}}^{\mathrm{opt},1}[k]$. Then, the MS uses this best hybrid combiner to transmit training sequence to the BS, where the BS looks for best hybrid precoder $\mathbf{F}_{\mathrm{T}}^{\mathrm{opt},1}[k]$ based on the received information. This process continues until the predefined maximum iterations M have been reached. Finally, the near-optimum pair of hybrid precoder and combiner as $\mathbf{F}_{\mathrm{T}}^{\mathrm{opt,m}}[k]$ and $\mathbf{W}_{\mathrm{R}}^{\mathrm{opt,m}}[k]$ are obtained. However, this procedure may take a longer time to converge to the global optimum due to randomly selected initial hybrid precoder or combiner. To tackle this problem, in the next subsection, we propose a simple solution based on EVD of the channel to calculate the initial hybrid precoder and combiner instead of randomly selecting from the codebook.

B. INITIAL HYBRID PRECODER OR COMBINER FOR TL-JOINT SEARCH

We utilize EVD of the channel to design the initial analog precoder and combiner based on the channel knowledge available at the BS or the MS. The phase of channel elements is extracted to design the analog precoder or combiner. Primarily, we have:

$$\bar{\mathbf{H}} = \frac{1}{K}\sum_{k=1}^{K}\mathbf{H}[k], \tag{12}$$

where $\bar{\mathbf{H}}$ is the sum of channels over all subcarriers. The procedure to obtain the analog precoder based on EVD can be expressed as:

Let, $\mathbf{P} = \bar{\mathbf{H}}^{H}\bar{H}$, where $\mathbf{P} \in \mathbb{C}^{N_{\mathrm{T}}\times N_{\mathrm{T}}}$ is a Hermitian and diagonalizable matrix. We decompose $\mathbf{P}$ by using EVD and then select the eigenvector $\mathbf{u}_{N_{\mathrm{T}}}$ corresponding to the largest

eigenvalue. $\mathbf{P}$ can be decomposed as $\mathbf{P} = \mathbf{U}\Lambda\tilde{\mathbf{H}}^H$, where the diagonal elements of matrix Λ present the eigenvalues Ψ_{N_T}, and each column of $\mathbf{U}$ is an eigenvector of $\mathbf{P}$. Then, $\mathbf{P}$ consists of N_T linear independent eigenvectors such that $\mathbf{u}_1, \mathbf{u}_2, \ldots, \mathbf{u}_{N_\mathrm{T}}$ where $\mathbf{u}_{N_\mathrm{T}} \in \mathbb{C}^{N_\mathrm{T}\times 1}$ with corresponding eigenvalues of $\Psi_1, \Psi_2, \ldots, \Psi_{N_\mathrm{T}}$, and $\mathbf{P}\mathbf{u}_i = \Psi_i\mathbf{u}_i$ for $i = 1, \ldots N_\mathrm{T}$. To design the analog precoder after decomposing $\mathbf{P}$, it selects the eigenvector corresponding to the largest eigenvalue in order to extract the phases of that vector which can be written as:

$$\mathbf{f}_{\mathrm{RF}} = \frac{1}{\sqrt{N_\mathrm{T}}} e^{j\arg[\mathbf{u}_1]}, \tag{13}$$

where $\mathbf{u}_1$ is the vector that is associated with the largest eigenvalue.[1]

After obtaining the initial analog precoder or combiner ($\mathbf{F}_{\mathrm{RF}}$ or $\mathbf{W}_{\mathrm{RF}}$) by EVD, the digital precoders and combiners are designed based on singular value decomposition (SVD). We define the effective baseband channel $\mathbf{H}_{\mathrm{eff}}[k]$ as:

$$\mathbf{H}_{\mathrm{eff}}[k] = (\mathbf{W}_{\mathrm{RF}})^H \mathbf{H}[k]\mathbf{F}_{\mathrm{RF}}. \tag{14}$$

For digital precoder and combiner, the SVD of the effective channel can be defined as:

$$\mathbf{H}_{\mathrm{eff}}[k] = \mathbf{U}[k]\Sigma[k]\mathbf{V}^H[k], \tag{15}$$

where $\mathbf{U}[k]$ and $\mathbf{V}[k]$ are $N_\mathrm{s} \times N_\mathrm{s}$ unitary matrices and Σ is a diagonal matrix of singular values $N_\mathrm{s} \times N_\mathrm{s}$. Then, we have SVD-based digital precoder and combiner as:

$$\mathbf{F}_{\mathrm{BB}}[k] = \mathbf{V}[k]. \tag{16}$$

$$\mathbf{W}_{\mathrm{BB}}[k] = \mathbf{U}[k]. \tag{17}$$

Finally, the digital precoder/combiner can be normalized as:

$$\mathbf{F}_{\mathrm{BB}}[k] = \frac{\sqrt{N_s}\mathbf{F}_{\mathrm{BB}}[k]}{\|\mathbf{F}_{\mathrm{RF}}\mathbf{F}_{\mathrm{BB}}[k]\|_F}. \tag{18}$$

$$\mathbf{W}_{\mathrm{BB}}[k] = \frac{\sqrt{N_s}\mathbf{W}_{\mathrm{BB}}[k]}{\|\mathbf{W}_{\mathrm{RF}}\mathbf{W}_{\mathrm{BB}}[k]\|_F}. \tag{19}$$

This enables us to assume $\mathbf{F}_{\mathrm{BB}}[k][\mathbf{F}_{\mathrm{BB}}[k]]^H \approx \mathbf{I}$ when $N_\mathrm{T}^{RF} = N_s$.

After the initial hybrid precoder $\mathbf{F}_\mathrm{T}^{\mathrm{opt},0}[k]$ for TL-joint search has been obtained, the best hybrid combiner $\mathbf{W}_\mathrm{R}^{\mathrm{opt},1}[k]$ at the MS can be searched by using the training sequence transmitted by the BS. Sequentially, this best hybrid combiner $\mathbf{W}_\mathrm{R}^{\mathrm{opt},1}[k]$ is used by the MS to send a training sequence to the BS so that the best hybrid precoder $\mathbf{F}_\mathrm{T}^{\mathrm{opt},1}[k]$ at the BS can be searched. This procedure of exchanging the training sequence between the BS and the MS continues for M maximum iterations. Finally, the near-optimum pair of hybrid precoder and combiner is obtained.

Note that in each iteration of TL-joint search, TS-algorithm is used to intelligently search the best hybrid precoder after the potential hybrid combiner is obtained. In the next section, the low-complexity TS-algorithm is explained in detail.

[1]The analog combiner can be obtained by following similar steps as described above by utilizing the channel knowledge available at the MS.

C. TABU-SEARCH ALGORITHM

In this section, we focus on searching the best hybrid precoder after the possible hybrid combiner has been obtained in TL-joint search by EVD.[2] The TS-algorithm can be expressed as follows.

TS-algorithm starts by selecting an arbitrary analog precoding matrix from the codebook $\mathcal{F}$. Then, based on neighboring criteria, it specifies several analog precoding matrices from the codebook $\mathcal{F}$ as the neighborhood around it. Next, it calculates the corresponding digital precoders by using the SVD of effective channel matrix. Finally, to select the starting point for the next iteration, it chooses the suitable solution between all the neighborhood despite the fact that the solution may not be global optimum [22]. However, selecting an arbitrary analog precoding matrix from codebook $\mathcal{F}$ as an initial solution may not be optimal due to the following reasons: 1) the problem is non-convex and only the local-optimum could be searched, or 2) due to the high dependence of global optimum on the initial point i.e., if the initial random solution is chosen far away from the real global-optimum point, the optimal solution might fail to obtain the global-optimum. Inspired by the above-mentioned reasons, we present a simple algorithm to obtain the initial analog precoder to start the TS-algorithm.

D. INITIAL HYBRID PRECODER/COMBINER FOR TS-ALGORITHM

Algorithm. 1 explains the basic idea to obtain the initial hybrid precoder and combiner from the codebooks ($\mathcal{F}$ and $\mathcal{W}$). At first, the BS analog precoder $\mathbf{f}_{\mathrm{RF}}$ and the MS analog combiner $\mathbf{w}_{\mathrm{RF}}$ vectors are jointly designed to maximize the desired signal power. As this is the typical single-user analog precoding/combining design problem, efficient beam training algorithms developed for the single-user system can be used. We utilize the idea in [13] to calculate the joint initial hybrid precoder and combiner for the TS-algorithm.

Algorithm 1 Initial Solution for TS-Algorithm

Input: $\mathcal{F}$ BS analog precoding codebook,
$\mathcal{W}$ MS analog combining codebook,

1: The BS and MS selects $\mathbf{v}^*$ and $\mathbf{g}^*$; that solve
2: $\{\mathbf{g}^*, \mathbf{v}^*\} \arg\max_{\substack{\forall g\in\mathcal{W}\\ \forall v\in\mathcal{F}}} \left\|\mathbf{g}^*\hat{\mathbf{H}}\mathbf{v}\right\|$;
3: MS sets $\mathbf{W}_{\mathrm{RF}} = \{\mathbf{g}_1^*, \mathbf{g}_2^*, \ldots, \mathbf{g}_{\mathrm{RF}}^*\}$;
4: BS sets $\mathbf{F}_{\mathrm{RF}} = \{\mathbf{v}_1^*, \mathbf{v}_2^*, \ldots, \mathbf{v}_{\mathrm{RF}}^*\}$;
5: Calculates corresponding digital prcoding/combining matrix at each subcarrier k by using (16)-(17);

Output: Initial hybrid precoder, Initial hybrid combiner;

Next, we specify the neighborhood around $\mathbf{F}_{\mathrm{RF}}$ from codebook $\mathcal{F}$ based on neighboring criteria. Then, we calculate the corresponding digital precoders at each subcarrier k by

[2]The process of searching the best hybrid combiner after a potential hybrid precoder has been obtained is similar.

using the effective channel matrix. For each selected neighborhood, we calculate K digital precoders to reflect that $\mathbf{F}_{\mathrm{RF}}$ is frequency-independent and remains unchanged for the whole wideband, whereas, the $\mathbf{F}_{\mathrm{BB}}[k]$ is frequency-selective and calculated at per-subcarrier basis, respectively. Finally, to get the starting point for the next iteration, our algorithm chooses the appropriate solution from all the neighborhood by calculating the cost function given in (10) (even if it is not the global optimum). This searching procedure will be continued until the predefined stopping criteria. Finally, the best solution is declared as the final solution.

V. IMPORTANT DEFINITIONS FOR TS-ALGORITHM

We start this section by discussing definitions of neighborhood, cost, Tabu, and stopping criteria and then, we analyze the complexity of the proposed scheme.

1) ***Defining Neighborhood****:* The gth column of $\mathbf{F}_{\mathrm{RF}}$ is shown by an index $z_g \in \left\{1, 2, \cdots, 2^{B_{\mathrm{T}}^{RF}}\right\}$, which corresponds to the vector $\mathbf{a}_{\mathrm{BS}}\left(\bar{\phi}_i^{\mathrm{BS}}\right)$ for $i = 1, \cdots, N_{\mathrm{T}}^{RF}$ at the BS and has $2^{B_{\mathrm{T}}^{RF}}$ possible candidates. Then, another analog precoder can be the neighbor of $\mathbf{F}_{\mathrm{RF}}$ if the following two conditions are satisfied:

1). The neighbor has b columns differentiating it from the corresponding columns in $\mathbf{F}_{\mathrm{RF}}$.

2). The difference in index between the two corresponding columns is equivalent to b.

Let $\mathbf{F}_{\mathrm{RF}}^{(j)}$ as the starting point for TS-algorithm in jth iteration, and $\mathcal{X}\left(\mathbf{F}_{\mathrm{RF}}^{(j)}\right) = \left\{\mathbf{X}_1^{(j)}, \mathbf{X}_2^{(j)}, \cdots, \mathbf{X}_{|\mathcal{X}|}^{(j)}\right\}$ is the neighborhood of $\mathbf{F}_{\mathrm{RF}}^{(j)}$, where $|\mathcal{X}|$ is the cardinality of $\mathcal{X}$.

To clearly understand this definition, let an analog precoder $\mathbf{F}_{\mathrm{RF}}^{(j)}$ defined as $\mathbf{F}_{\mathrm{RF}}^{(j)} = \left[\mathbf{a}_{\mathrm{BS}}\left(3\pi/4\right), \mathbf{a}_{\mathrm{BS}}\left(7\pi/4\right)\right]$ when $N_{\mathrm{T}}^{RF} = 2$, $2^{B_{\mathrm{T}}^{RF}} = 3$ and $b = 1$. Then, according to the above two definitions of neighborhood, it is clear that the cardinality $|\mathcal{X}| = 2N_{\mathrm{T}}^{RF}$. Therefore, $\mathbf{F}_{\mathrm{RF}}^{(j)}$ can have following neighborhood:

$$\begin{aligned}
\mathbf{X}_1^{(j)} &= \left[\mathbf{a}_{\mathrm{BS}}\left(2\pi/4\right), \mathbf{a}_{\mathrm{BS}}\left(7\pi/4\right)\right] \\
\mathbf{X}_2^{(j)} &= \left[\mathbf{a}_{\mathrm{BS}}\left(4\pi/4\right), \mathbf{a}_{\mathrm{BS}}\left(7\pi/4\right)\right] \\
\mathbf{X}_3^{(j)} &= \left[\mathbf{a}_{\mathrm{BS}}\left(3\pi/4\right), \mathbf{a}_{\mathrm{BS}}\left(6\pi/4\right)\right] \\
\mathbf{X}_4^{(j)} &= \left[\mathbf{a}_{\mathrm{BS}}\left(3\pi/4\right), \mathbf{a}_{\mathrm{BS}}\left(8\pi/4\right)\right]
\end{aligned}$$

2) ***Cost Computation****:* The cost function $\varphi(\mathbf{F}_{\mathrm{T}}[k], \mathbf{W}_{\mathrm{R}}[k])$ is defined as the reliability metric for the optimal hybrid precoder $\mathbf{F}_{\mathrm{T}}[k]$.

The hybrid precoder $\mathbf{F}_{\mathrm{T}}[k]$ which leads to the largest value of cost function $\varphi\left(\mathbf{F}_{\mathrm{T}}[k], \mathbf{W}_{\mathrm{R}}[k]\right)$ is a better solution. Moreover, according to [22], by the definition of the neighborhood, if the cost function of $\mathbf{F}_{\mathrm{T}}[k]$ is obtained once, we do not need to re-calculate the cost function of its neighbors by using the information exchange between the BS and the MS.

3) ***Tabu Definition****:* The definition of "tabu" is criteria dependent and can thus be changed accordingly. Generally, the tabu is well-defined as "move" which specifies the direction of a solution (i.e., from one solution to another). TS attempts to escape from the local optimum by utilizing the concept of "tabu", the definition of which can be changed according to different criteria such as convergence speed, complexity and several others. The "move" is shown as (a,b), where $a = 1, \ldots, N_{\mathrm{T}}^{RF}$ represents that the ath column in the original solution is distinct from the current solution. Whereas, $b \in \{-1, 1\}$ shows the changed index of this specific column from the original solution to the current solution.

To further explain the "move", consider the following example, where move from $\left[\mathbf{a}_{BS}\left(2\pi/4\right), \mathbf{a}_{BS}\left(7\pi/4\right)\right]$ to $\left[\mathbf{a}_{BS}\left(3\pi/4\right), \mathbf{a}_{BS}\left(7\pi/4\right)\right]$ can be written as $(1, +1)$.

In some cases, the cost function of the same neighbor is computed again if it is searched in another iteration. To avoid this problem, we utilize the same idea proposed in [22] to calculate the index of each candidate analog precoder.

Let $p = 1, 2, \ldots, 2^{B_{\mathrm{T}}^{RF}.N_{\mathrm{T}}^{RF}}$ is the index of the candidate analog precoder out of $\mathcal{F}$ with $2^{B_{\mathrm{T}}^{RF}.N_{\mathrm{T}}^{RF}}$ possible entries. Then, p can be be calculated as:

$$p = \sum_{g=1}^{N_{\mathrm{T}}^{RF}} \left(z_g - 1\right)\left(2^{B_{\mathrm{T}}^{RF}}\right)^{N_{\mathrm{T}}^{RF}-g} + 1. \tag{20}$$

In this way, we can effectively avoid a solution for being searched twice and hence, provide a better and wide search range.

4) ***Stopping Criterion****:* We define two conditions to terminate the TS-algorithm.

1) The predefined maximum iterations max_iter meet the total number of iterations.

2) The global optimum-solution count (i.e., global solution not being updated flag = max_len) meets the maximum predefined value max_len.

The flag is defined to indicate how long the global optimum solution has not been updated. For example, flag = flag + 1, if the starting point is sub-optimal for the next iteration, otherwise flag = 0 indicates that the global-solution is selected for the next iteration.

5) ***TS-based Joint Hybrid Precoding/Combining****:* Pseudo code of the proposed algorithm is presented in **Algorithm 2**. Here, we explain some of the important steps in detail.

Let $\mathbf{G}^{(j)}[k]$ be the hybrid precoder that has achieved the maximum cost function (10) until the jth iteration. The TS-based joint hybrid precoding/combining begins by calculating initial hybrid precoder $\mathbf{F}_{\mathrm{T}}^{(0)}[k]$ using **Algorithm. 1**. For this initial solution, we set $\mathbf{G}^{(j)}[k] = \mathbf{F}_{\mathrm{T}}^{(0)}[k]$, flag = 0, and $\mathbf{t} = 0$ where $\mathbf{t}$ is the tabu list.

Step 1*:* Compute the cost function (10) of $2N_{\mathrm{T}}^{RF}$ neighbors of $\mathbf{F}_{\mathrm{T}}^{j}[k]$ by using the effective channel matrix $(\mathbf{W}_{\mathrm{R}}[k])^{H}\mathbf{H}[k]\mathbf{F}_{\mathrm{T}}^{(j)}[k]$. Let,

$$\mathbf{X}_{\mathrm{T}}^{1}[k] = \arg \max_{1 \le u \le 2N_{\mathrm{T}}^{RF}} \varphi\left(\mathbf{X}_{\mathrm{T}}^{u}[k], \mathbf{W}_{\mathrm{R}}[k]\right) \tag{21}$$

Calculate the index p^1 of $\mathbf{X}_{\mathrm{T}}^{1}[k]$ in codebook $\mathcal{F}$ according to (20). The $\mathbf{X}_{\mathrm{T}}^{1}[k]$ can be selected as the next iteration starting point if either of the subsequent conditions is

Algorithm 2 TS-Based Hybrid Joing Precoding/Combining

Input: $\mathcal{F}$ BS analog precoding codebook, $\mathcal{W}$ MS analog combining codebook, $\mathbf{G}^{(i)}[k]$; $\mathbf{H}[k]$; $flag = 0$; $\mathbf{t} = 0$; Search interval b; Iteration number J;

1: **for** j = 0; $j < J$; $j++$ **do**
2: Calculate the initial hybrid precoder using **Algorithm 1**;
3: Define the $2N_{\mathrm{T}}^{RF}$ neighborhood;
4: Calculate digital preocders $\mathbf{F}_{\mathrm{BB}}[k]$ at each subcarrier k according to (15);
5: Calculate the cost function according to (10);
6: Calculate the index $\mathbf{p}'$ according to (20);
7: Calculate $\mathbf{X}'_{\mathrm{T}}[k]$ satisfies (22) and (23);
8: Set next starting point as $\mathbf{F}_{\mathrm{T}}^{(j+1)}[k] = \mathbf{X}'_{\mathrm{T}}[k]$;
9: Set new search according to (25);
10: **end for**;

Output: near-optimal hybrid precoder $\mathbf{F}_{\mathrm{T}}[k]$;

fulfilled.

$$\varphi\left(\mathbf{X}_{\mathrm{T}}^{1}[k], \mathbf{W}_{\mathrm{R}}[k]\right) > \varphi\left(\mathbf{G}^{(j)}[k], \mathbf{W}_{\mathrm{R}}[k]\right) \quad (22)$$

$$\mathbf{t}(p') = 0 \quad (23)$$

If $\mathbf{X}_{\mathrm{T}}^{1}[k]$ fails to satisfy the two conditions, we obtain the 2nd better solution as:

$$\mathbf{X}_{\mathrm{T}}^{2}[k] = \arg \max_{1 \le u \le 2N_{\mathrm{T}}^{RF}} \varphi\left(\mathbf{X}_{\mathrm{T}}^{v}[k], \mathbf{W}_{\mathrm{R}}[k]\right) \quad (24)$$

$\mathbf{X}_{\mathrm{T}}^{2}[k]$ can be used for next iteration's starting point if it satisfies the conditions (22) and (23), respectively. We continue this procedure until the appropriate solution among all the neighbors $\mathbf{X}'_{\mathrm{T}}[k]$ is selected as the next iteration's starting point. If no solution satisfies (22) and (23), the same process is repeated by setting tabu list $t = 0$.

Step 2: From the solution obtained in step 1 as the starting point for the next iteration (i.e., $\mathbf{F}_{\mathrm{T}}^{(j+1)}[k] = \mathbf{X}'_{\mathrm{T}}[k]$), we set,

$$\begin{cases} \mathbf{t}'(p) = 0, & \mathbf{G}^{(j+1)}[k] = \mathbf{F}_{T}^{(j+1)}[k], \\ & \text{if } \varphi\left(\mathbf{F}_{T}^{(j+1)}[k], \mathbf{W}_{R}[k]\right) \\ & > \varphi\left(\mathbf{G}^{j}[k], \mathbf{W}_{R}[k]\right), \\ \mathbf{t}'(p) = 1, & \mathbf{G}^{(j+1)}[k] = \mathbf{G}^{j}[k], \\ & \text{if } \varphi\left(\mathbf{F}_{T}^{(j+1)}[k], \mathbf{W}_{R}[k]\right) \\ & \leqslant \varphi\left(\mathbf{G}^{j}[k], \mathbf{W}_{R}[k]\right), \end{cases} \quad (25)$$

If the stopping criterion is satisfied in *Step 2*, the TS-algorithm will be terminated and it outputs the final solution as $\mathbf{G}^{(\mathrm{j}+1)}[k]$. Else, the algorithm continues to repeat *step 1* until it meets the certain stopping criterion. It should be emphasized after best hybrid precoder $\mathbf{F}_{\mathrm{T}}[k]$ has been obtained, the procedure to search the best hybrid combiner $\mathbf{W}_{\mathrm{R}}[k]$ is similar to the process of selecting the best hybrid precoder.

A. COMPLEXITY ANALYSIS

In this section, the complexity analysis of the proposed TS-based joint hybrid precoding and combining is presented and compared with conventional full search (FS)-based hybrid precoding [17]. It is worth pointing out although the proposed Turbo-TS beamforming requires some extra information exchange between the BS and the UE (M times of iterations) as discussed in Section III-B, the corresponding overhead is trivial compared to the searching complexity, since K is usually small (e.g., $M = 3$ as will be verified by the simulation results). Therefore, in this section, we evaluate the complexity as the total number of solutions needed to be searched. The complexity of the proposed scheme is divided into two parts: (i) the initial solution, and (ii) the TS-algorithm.

i). From **Algorithm 1**, it can be observed that the complexity of this part is dominated by the EVD of $\mathbf{P} = \bar{\mathbf{H}}^{H}\bar{\mathbf{H}}$. Therefore, the complexity of this initial part can be written as:

$$C_{\mathrm{ini}} = \mathcal{O}\left(N_{T}^{3}\right). \quad (26)$$

If we define n as the index of EVD repetition in the proposed solution, then (26) can be written as

$$C_{\mathrm{ini}} = \mathcal{O}\left(n * N_{T}^{3}\right). \quad (27)$$

The remaining part is the selection process which has a very low-complexity and thus can be ignored.

ii). The parameter to evaluate the complexity of TS-algorithm is the total number of solutions required to be searched. The searching complexity of TS-algorithm is given by:

$$C_{\mathrm{TS}} = \left(2N_{\mathrm{T}}^{RF}\,\mathrm{max\_iter} + 2N_{\mathrm{R}}^{RF}\,\mathrm{max\_iter}\right)M, \quad (28)$$

In comparison, the searching complexity of FS-based hybrid precoding is as follows:

$$C_{\mathrm{FS}} = K\binom{N_{\mathrm{T}}^{RF}}{2^{B_{\mathrm{T}}^{RF}}} \times K\binom{N_{\mathrm{R}}^{RF}}{2^{B_{\mathrm{R}}^{RF}}}, \quad (29)$$

By comparing (28) and (29), we observe that the complexity of TS-based joint hybrid precoding and combining is linear with N_{T}^{RF} and N_{R}^{RF}, and it does not depend on B_{R}^{RF} and B_{T}^{RF}, respectively. Hence, the proposed solution has lower-complexity as compared to FS-based hybrid precoding.

VI. SIMULATION RESULTS

We evaluate the achievable sum-rate of the proposed TS-based joint hybrid precoding and combining in this section. To validate the proposed scheme, we compare it with some existing hybrid precoding schemes [21] and [17] proposed for wideband mmWave massive MIMO systems. The simulation parameters are defined as follows.

The channel model is generated as presented in [20], where the AoAs/AoDs follows a uniform distribution between $[0, 2\pi]$. The lth path complex gain α_l follows $\alpha_l \sim \mathcal{CN}(0, 1)$, and the total number of propagation path is set to $L = 5$, where each cluster has $R_l = 3$ rays with Laplacian distributed

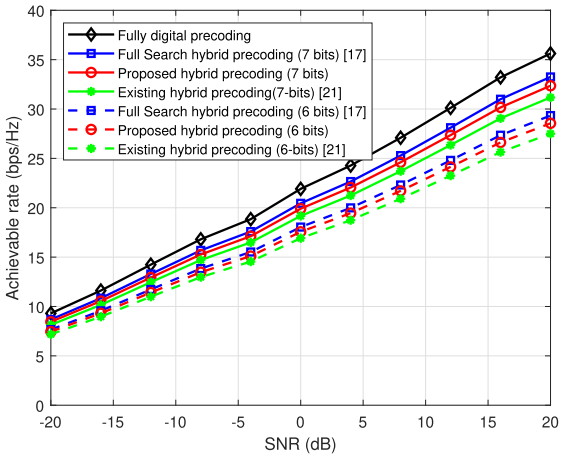

FIGURE 3. Achieveable sum-rate comparison of different hybrid precoding schemes when $N_{\mathrm{R}} \times N_{\mathrm{T}} = 16 \times 64$ and $N_{\mathrm{R}}^{RF} = N_{\mathrm{T}}^{RF} = N_s = 2$.

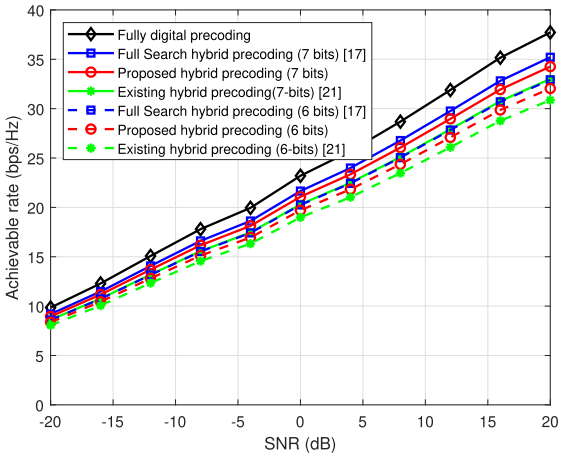

FIGURE 4. Achievable sum-rate comparison of different hybrid precoding schemes when $N_{\mathrm{R}} \times N_{\mathrm{T}} = 32 \times 128$ and $N_{\mathrm{R}}^{RF} = N_{\mathrm{T}}^{RF} = N_s = 2$.

AoAs/AoDs [10], respectively. The carrier-frequency is set to 60 GHz. Likewise, the number of subcarriers and the system bandwidth are set to $K = 128$ and 4 GHz, respectively. At the BS and the MS, ULA with antenna spacing $d_s = \lambda/2$ is implemented. For the quantified bits per AoA/AoD, two cases are considered, i.e., $B_{\mathrm{T}}^{RF} = B_{\mathrm{R}}^{RF} = 7$, and $B_{\mathrm{T}}^{RF} = B_{\mathrm{R}}^{RF} = 6$. Finally, the SNR is defined as ρ/σ^2.

At first, the perfect channel-state-information (CSI) scenario is considered. In Fig. 3, we compare the achievable sum-rate of the proposed solution with conventional FS-based hybrid precoding [17] and the hybrid precoding [21]. We set an arrangement of $N_{\mathrm{R}} \times N_{\mathrm{T}} = 16 \times 64$ antennas having $N_{\mathrm{R}}^{RF} = N_{\mathrm{T}}^{RF} = N_{\mathrm{s}} = 2$.

Fig. 3 clearly shows the proposed scheme can obtain the sum-rate very close to FS-based hybrid precoding. For instance, when $B_{\mathrm{T}}^{RF} = B_{\mathrm{R}}^{RF} = 6$ and SNR = 0dB, the sum-rate achieved by the proposed scheme is very close to the sum-rate obtained by FS-based hybrid precoding. Further the achievable sum-rate of the proposed solution is higher than the hybrid precoding scheme because in our solution the hybrid precoder and combiner are jointly optimized. In contrast, the hybrid precoding algorithm does not take into account the hybrid combiner while optimizing the hybrid precoder.

Further, by increasing the number of quantified bits per AoA/AoD, i.e., when $B_{\mathrm{T}}^{RF} = B_{\mathrm{R}}^{RF} = 7$ instead of 6, the performance gap between the fully digital precoding and the proposed scheme becomes smaller. Therefore, we conclude here the proposed solution can achieve the sum-rate very close to the conventional FS-based hybrid precoding with $B_{\mathrm{T}}^{RF} = B_{\mathrm{R}}^{RF} = 7$ and its performance is better than the hybrid precoding scheme in [21].

In Fig. 4, we repeat the same sum-rate comparison with a different antenna setting such as $N_{\mathrm{R}} \times N_{\mathrm{T}} = 32 \times 128$ having $N_{\mathrm{R}}^{RF} = N_{\mathrm{T}}^{RF} = N_{\mathrm{s}} = 2$.

Clearly, Fig. 4 shows similar trends as Fig. 3 in terms of achievable sum-rate. It is worth mentioning here by increasing the number of antennas at the BS and the MS, the achievable sum-rate is also increased from 31 bits/s/Hz to 34 bits/s/Hz compared to Fig. 3. Therefore, we observe here that increasing the low-cost antennas has a positive impact on the sum-rate of the proposed scheme instead of increasing expensive RF chains, respectively.

It is important to show the effect of imperfect CSI to observe the generality of the proposed solution in other scenarios. The estimated channel matrix $\hat{\mathbf{H}}[k]$ can be modeled as [25],

$$\hat{\mathbf{H}}[k] = \xi \mathbf{H}[k] + \sqrt{1-\xi^2}\mathbf{E}, \tag{30}$$

where $\mathbf{H}[k]$ is the actual channel matrix. CSI accuracy is presented as $\xi \in [0, 1]$, and $\mathbf{E}$ is the error matrix the entries of which follow i.i.d as $\mathcal{CN}(0, 1)$, respectively.

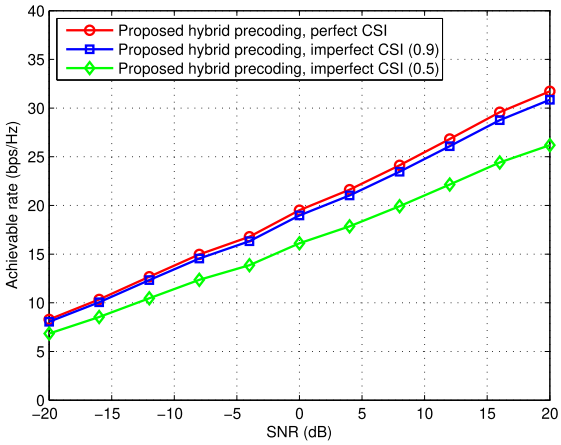

FIGURE 5. Impact of imperfect CSI on proposed hybrid precoding when $N_r \times N_t = 16 \times 64$ antennas and $N_r^{RF} = N_t^{RF} = N_s = 2$ RF chains.

We set $N_{\mathrm{R}} \times N_{\mathrm{T}} = 16 \times 64$ and $N_{\mathrm{R}}^{RF} = N_{\mathrm{T}}^{RF} = N_{\mathrm{s}} = 2$ for Fig. 5 to observe the imperfect CSI effect. Clearly the proposed solution is not very sensitive to CSI-accuracy. For instance, when the CSI-accuracy is 90%, the proposed approach achieves a sum-rate very close to perfect-CSI scenario. Further, when the CSI-accuracy is poor i.e., 50%, our scheme maintains 85% of the sum-rate achieved in perfect CSI-scenario.

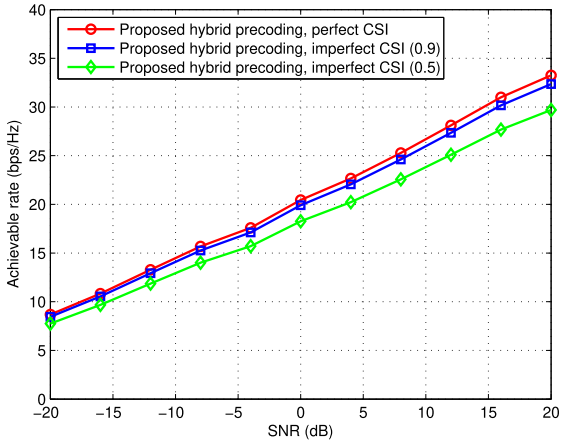

FIGURE 6. Impact of imperfect CSI on proposed hybrid precoding when $N_r \times N_t = 32 \times 128$ antennas and $N_r^{RF} = N_t^{RF} = N_s = 2$ RF chains.

In Fig. 6, the imperfect-CSI comparison is extended for different antenna numbers such that $N_{\mathrm{R}} \times N_{\mathrm{T}} = 128 \times 32$ having $N_{\mathrm{R}}^{RF} = N_{\mathrm{T}}^{RF} = N_{\mathrm{s}} = 2$, respectively. However, the same conclusions can be drawn as those in Fig. 5.

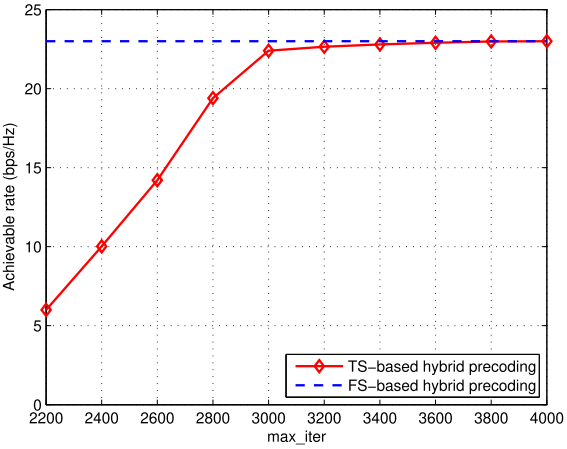

FIGURE 7. Achievable sum-rate of TS-based joint hybrid precoding/combining scheme against max_iter.

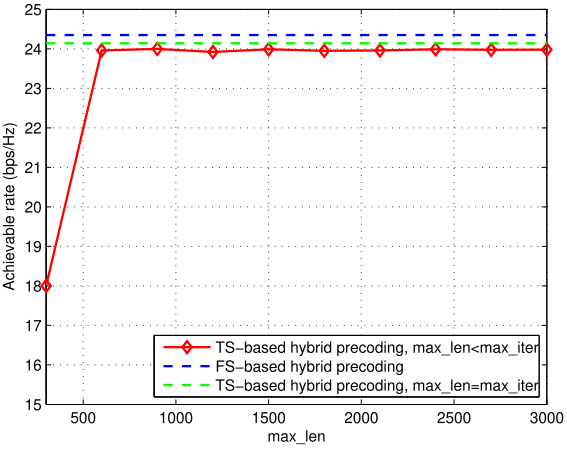

FIGURE 8. Achievable sum-rate of TS-based joint hybrid precoding/combining scheme against max_len.

Fig. 7 shows the achievable sum-rate of TS-based joint hybrid precoding and combining against the pre-defined maximum number of iterations max_iter. The simulation parameters are set as: $N_{\mathrm{R}} \times N_{\mathrm{T}} = 16 \times 64$, $N_{\mathrm{R}}^{RF} = N_{\mathrm{T}}^{RF} = N_{\mathrm{s}} = 2$, SNR $= 0$ dB, $M = 3$, and max_len $=$ max_iter, respectively. From Fig. 1, we can observe the achievable rate of the proposed Turbo-TS beamforming can be improved by increasing *max_iter*. More importantly, when *max_iter* is large enough, Turbo-TS beamforming can converge to the conventional full-search (FS) beamforming without performance loss.

Fig. 8 shows the achievable sum-rate comparison of max_len, where max_iter is fixed to 3000. Other simulation parameters are same as those for Fig. 3. The figure shows when max_len is small, the TS-based joint hybrid precoding and combining falls into the local optimum, leading to serious performance loss. However, when max_len becomes large (e.g., max_len $= 600$), the proposed scheme effectively escapes from the local optimum and achieves exact performance when max_iter $=$ max_len. This observation indicates although we set max_len $<$ max_iter to further reduce the searching complexity, the optimum performance of the proposed scheme can still be guaranteed.

VII. CONCLUSION

This paper presents the TS-based joint hybrid precoding and combining scheme for wideband mmWave massive MIMO systems to maximize the achievable sum-rate. At first, we develop a TL-joint search by using the idea of iterative information exchange between the BS and the MS. Then, TS-algorithm is utilized in each iteration of TL-joint searching to find the best pair of hybrid precoder and combiner with low-complexity. Our analyses has allowed us to calculate the linear-complexity of the proposed solution. The simulation results verify the better sum-rate performance of our scheme compared to traditional solutions for wideband mmWave massive MIMO systems. Our future work will focus on extending the proposed Turbo-TS beamforming to the multi-user scenario.

REFERENCES

[1] Z. Wang, M. Li, Q. Liu, and A. L. Swindlehurst, "Hybrid precoder and combiner design with low-resolution phase shifters in mmWave MIMO systems," *IEEE J. Sel. Topics Signal Process.*, vol. 12, no. 2, pp. 256–269, May 2018.
[2] Z. Pi and F. Khan, "An introduction to millimeter-wave mobile broadband systems," *IEEE Commun. Mag.*, vol. 49, no. 6, pp. 101–107, Jun. 2011.
[3] S. Mumtaz, J. Rodriguez, and L. Dai, *mmWave Massive MIMO: A Paradigm for 5G*. New York, NY, USA: Academic, 2016.
[4] A. Alkhateeb, J. Mo, N. Gonzalez-Prelcic, and R. W. Heath, "MIMO precoding and combining solutions for millimeter-wave systems," *IEEE Commun. Mag.*, vol. 52, no. 12, pp. 122–131, Dec. 2014.
[5] X. Gao, L. Dai, and A. M. Sayeed, "Low RF-complexity technologies to enable millimeter-wave MIMO with large antenna array for 5G wireless communications," *IEEE Commun. Mag.*, vol. 56, no. 4, pp. 211–217, Apr. 2018.
[6] L. Wei, R. Hu, Y. Qian, and G. Wu, "Key elements to enable millimeter wave communications for 5G wireless systems," *IEEE Wireless Commun.*, vol. 21, no. 6, pp. 136–143, Dec. 2014.
[7] P. Dong, H. Zhang, and G. Y. Li, "Framework on deep learning-based joint hybrid processing for mmWave massive MIMO systems," *IEEE Access*, vol. 8, pp. 106023–106035, 2020.

[8] L. N. Ribeiro, S. Schwarz, M. Rupp, and A. L. F. de Almeida, "Energy efficiency of mmWave massive MIMO precoding with low-resolution DACs," *IEEE J. Sel. Topics Signal Process.*, vol. 12, no. 2, pp. 298–312, May 2018.

[9] X. Gao, L. Dai, S. Han, C.-L. I, and R. W. Heath, "Energy-efficient hybrid analog and digital precoding for mmWave MIMO systems with large antenna arrays," *IEEE J. Sel. Areas Commun.*, vol. 34, no. 4, pp. 998–1009, Apr. 2016.

[10] O. E. Ayach, S. Rajagopal, S. Abu-Surra, Z. Pi, and R. W. Heath, "Spatially sparse precoding in millimeter wave MIMO systems," *IEEE Trans. Wireless Commun.*, vol. 13, no. 3, pp. 1499–1513, Mar. 2014.

[11] E. E. Bahingayi and K. Lee, "Low-complexity incremental search-aided hybrid precoding and combining for massive MIMO systems," *IEEE Access*, vol. 8, pp. 66867–66877, 2020.

[12] Z. Cheng, Z. Wei, and H. Yang, "Low-complexity joint user and beam selection for beamspace mmWave MIMO systems," *IEEE Commun. Lett.*, vol. 24, no. 9, pp. 2065–2069, Sep. 2020.

[13] X. Zhang, A. F. Molisch, and S.-Y. Kung, "Variable-phase-shift-based RF-baseband codesign for MIMO antenna selection," *IEEE Trans. Signal Process.*, vol. 53, no. 11, pp. 4091–4103, Nov. 2005.

[14] X. Yu, J.-C. Shen, J. Zhang, and K. B. Letaief, "Alternating minimization algorithms for hybrid precoding in millimeter wave MIMO systems," *IEEE J. Sel. Topics Signal Process.*, vol. 10, no. 3, pp. 485–500, Apr. 2016.

[15] J. Singh and S. Ramakrishna, "On the feasibility of codebook-based beamforming in millimeter wave systems with multiple antenna arrays," *IEEE Trans. Wireless Commun.*, vol. 14, no. 5, pp. 2670–2683, May 2015.

[16] M. Kim and Y. H. Lee, "MSE-based hybrid RF/baseband processing for millimeter-wave communication systems in MIMO interference channels," *IEEE Trans. Veh. Technol.*, vol. 64, no. 6, pp. 2714–2720, Jun. 2015.

[17] S. Hur, T. Kim, D. J. Love, J. V. Krogmeier, T. A. Thomas, and A. Ghosh, "Millimeter wave beamforming for wireless backhaul and access in small cell networks," *IEEE Trans. Commun.*, vol. 61, no. 10, pp. 4391–4403, Oct. 2013.

[18] T. Mir, M. Zain Siddiqi, U. Mir, R. Mackenzie, and M. Hao, "Machine learning inspired hybrid precoding for wideband millimeter-wave massive MIMO systems," *IEEE Access*, vol. 7, pp. 62852–62864, 2019.

[19] R. Zhang, W. Hao, G. Sun, and S. Yang, "Hybrid precoding design for wideband THz massive MIMO-OFDM systems with beam squint," *IEEE Syst. J.*, early access, Jul. 1, 2020, doi: 10.1109/JSYST.2020.3003908.

[20] A. Alkhateeb and R. W. Heath, "Frequency selective hybrid precoding for limited feedback millimeter wave systems," *IEEE Trans. Commun.*, vol. 64, no. 5, pp. 1801–1818, May 2016.

[21] S. Park, A. Alkhateeb, and R. W. Heath, "Dynamic subarrays for hybrid precoding in wideband mmWave MIMO systems," *IEEE Trans. Wireless Commun.*, vol. 16, no. 5, pp. 2907–2920, May 2017.

[22] X. Gao, L. Dai, C. Yuen, and Z. Wang, "Turbo-like beamforming based on tabu search algorithm for millimeter-wave massive MIMO systems," *IEEE Trans. Veh. Technol.*, vol. 65, no. 7, pp. 5731–5737, Jul. 2016.

[23] T. Kim, J. Park, J.-Y. Seol, S. Jeong, J. Cho, and W. Roh, "Tens of gbps support with mmWave beamforming systems for next generation communications," in *Proc. IEEE Global Commun. Conf. (GLOBECOM)*, Dec. 2013, pp. 3685–3690.

[24] J. Wang, Z. Lan, C.-W. Pyo, T. Baykas, C.-S. Sum, M. A. Rahman, J. Gao, R. Funada, F. Kojima, H. Harada, and S. Kato, "Beam codebook based beamforming protocol for multi-gbps millimeter-wave WPAN systems," *IEEE J. Sel. Areas Commun.*, vol. 27, no. 8, pp. 1390–1399, Oct. 2009.

[25] F. Rusek, D. Persson, B. K. Lau, E. G. Larsson, T. L. Marzetta, O. Edfors, and F. Tufvesson, "Scaling up MIMO: Opportunities and challenges with very large arrays," *IEEE Signal Process. Mag.*, vol. 30, no. 1, pp. 40–60, Jan. 2013.

TALHA MIR (Member, IEEE) received the B.S. degree in electronic engineering from the Balochistan University of Information Technology, Engineering, and Management Sciences (BUITEMS), Pakistan, in 2007, the master's degree from the University of Bradford, England, in 2011, and the Ph.D. degree from Tsinghua University, Beijing, China, in 2020. He is currently an Assistant Professor with the Electrical Engineering Department, BUITEMS. His research interests include resource wireless communications and networking, next generation networks, massive multiple-input multiple-output, mm-waves, and spatial movements.

UBAID ABBASI received the M.S. degree from SUPELEC, Rennes, France, in 2008, and the Ph.D. degree from the University of Bordeaux, France, in 2012. He was a Senior Research Fellow with the University of Quebec, Montreal. He is currently an Assistant Professor with the Department of Sciences, GPRC, Grande Prairie, AB, Canada. He also works on Project funded by Ericsson Canada. His research interests include inter-container communications, data center communication issues, device to device communication in next generation 5G networks, wireless communications, and big data analysis.

RAZA ALI (Member, IEEE) received the B.S. degree in telecommunication engineering from the Balochistan University of Information Technology, Engineering, and Management Sciences, Pakistan, in 2009, and the master's degree in electrical engineering from the University of Engineering and Technology Lahore, Pakistan, in 2015. He has been a Faculty Member with the Faculty of Information and Communication Technology, BUITEMS, since January 2013. He is currently a Ph.D. Researcher with the VIP Laboratory, University of Malaya, Malaysia. He is also a coordinator for awards and grants with the IEEE Malaysia SAC. His research interests include image processing, computer vision, and deep learning for semantic segmentation.

SYED MUDASSIR HUSSAIN (Member, IEEE) received the B.S. and M.S. degrees in electronic engineering from the Balochistan University of Information Technology Engineering, and Management Sciences (BUITEMS), Quetta, Pakistan, in 2010 and 2015, respectively. He is currently pursuing the Ph.D. degree with the Department of Microelectronics and Nanoelectronics, Tsinghua University, Beijing, China. Since 2011, he has been with the Department of Electronic Engineering, BUITEMS. He is also an Assistant Professor. His ongoing research is about SoC design for a visual aided system for total hip arthroplasty surgeries. His research interests include integrated circuit designs and digital image processing.

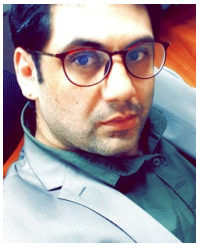

USAMA MIR (Senior Member, IEEE) received the B.S. degree (Hons.) in computer engineering from the Balochistan University of Information Technology, Engineering, and Management Sciences, Pakistan, in 2006, and the master's and Ph.D. degrees in computer science from the University of Technology of Troyes, France, in 2008 and 2011, respectively. He was a Postdoctoral Fellow with Telecom Bretagne, France, from 2011 to 2012. He was the Head of the Electronics Engineering Department, Iqra University Islamabad, Pakistan, from 2012 to 2015. He is currently an Assistant Professor with the Department of Computing and IT, Saudi Electronic University, Saudi Arabia. His research interests include big data analysis, blockchains, multiple-input multiple-output technology, resource allocation and handoff management in cognitive radio systems, bitcoin and digital currencies, wireless communications and networking, and multiagent systems. He serves as an Associate Editor for IEEE Access.